

Effect of Carbon–Fluorine Additive to a Flux on the Metal Structure of the Electric Arc Surfacing of a Low-Alloy Wire

Yu. F. Ivanov^{a, *}, R. E. Kryukov^b, V. E. Gromov^{b, **}, N. A. Kozyrev^b, and Yu. A. Shliarova^b

^a Institute of High Current Electronics, Siberian Branch, Russian Academy of Sciences, Tomsk, 634055 Russia

^b Siberian State Industrial University, Novokuznetsk, 654007 Russia

*e-mail: yufi55@mail.ru

**e-mail: gromov@physics.sibsiu.ru

Received January 14, 2022; revised March 12, 2022; accepted March 12, 2022

Abstract—The effect of a carbon–fluorine containing additive to the flux from silicomanganese slag with a low content of manganese oxide on the structural and phase state, defects, and fracture surface of the electric arc surfacing of low-carbon steel is investigated using transmission- and scanning-electron microscopy. A quantitative analysis of the parameters of the structure, phase composition, and dislocation substructure of the surfacings formed with and without additives to the flux is carried out. It is shown that the deposited metal with the additive to the flux has a layered structure. It is revealed that the predominant mechanism of surfacing failure is ductile fracture with the formation of a pitted fracture structure. Regions of quasi-brittle fracture are found much less frequently. The main structural component of the surfacing metal are grains of the α phase of the surfacing metal. The second structural component of the surfacing are pearlite grains of lamellar morphology, the relative content of which in the surfacing with carbon–fluorine containing additive to the flux is three times higher than in the surfacing without the additive to the flux. In most cases, the grains of the α phase are fragmented. Rounded iron-carbide particles with a size from 20 to 80 nm are found in the grains of the α phase of the surfacing metal with a carbon–fluorine containing additive to the flux. The surfacing metal with the additive to the flux is characterized by higher values of the scalar and excess dislocation density, and amplitude of curvature–torsion of the crystal lattice. It is concluded that the use of a carbon–fluorine containing additive in the flux during the formation of a surfacing will affect the mechanical properties.

Keywords: surfacing, structure, phase composition, dislocations, fracture surface, addition to the flux

DOI: 10.1134/S1027451022060398

INTRODUCTION

Machine parts and mechanisms of the equipment of mining, construction, and metallurgical industries experiencing extreme mechanical and cyclic impacts, wear, and corrosion prematurely fail, which causes the need for repair and restoration work. The task of increasing the reliability and durability is currently being solved by purposeful changes in the properties of the working surfaces of machine parts and mechanisms. Surface coatings with high performance parameters are created using a core wire containing hard alloys and chemical compounds [1–5]. This process depends on the operating conditions of the products. Another promising direction for improving the operating properties of deposited materials is the use of carbon-containing additives in the fluxes and core wires [6–10]. The role of carbon-containing additives in the formation of the structural and phase states, defects, and fracture surface of a surfacing from low-carbon steel is analyzed in [11, 12]. For an informed choice of the flux material and additives to it when

creating surfacings that ensure the obtaining of a complex of physical and mechanical properties of the surfacing structures required by regulatory documents, it is necessary to carry out detailed studies using methods of modern physical material science of the structural and phase states and features of the destruction of the surfacing material. This is the aim of the present study.

MATERIALS AND METHODS

Samples obtained by electric-arc surfacing using an Sv-08GA wire under a flux layer of silicomanganese slag with a low content of manganese oxide were used as the research material (Table 1) without an additive (sample no. 1) and with an FD-UFS carbon–fluorine containing additive (Table 2) in an amount of 6 wt % (sample no. 2). The process was carried out using an ASAW-1200 setup at a current of 700 A, voltage of 30 V, and surfacing speed of 30 m/min. The structure of the surfacing metal was studied using scanning

Table 1. Chemical composition of the flux, wt %

FeO	MnO	CaO	SiO	Al ₂ O ₃	MgO	S	P	ZnO	C	F	TiO ₂	Cr ₂ O ₃
0.70	6.69	27.99	35.96	14.96	8.02	0.64	0.021	0.013	0.020	0.14	0.22	0.052

Table 2. Chemical composition of the carbon–fluorine containing additive of FD-UFS brand, wt %

Fe ₂ O ₃	MnO	Ca	SiO ₂	Al	MgO	Na	K	F	C	S	P
1.67	0.03	0.74	25.49	12.28	0.13	17.5	12.48	15.06	13.97	0.15	0.05

microscopy (SEM) (LEO EVO50 and MIRA3 Tescan instruments) and transmission electron diffraction microscopy (TEM) (JEOL JEM2100 instrument) [13–15]. The objects of the study for SEM were prepared using two methods. The first method of preparing the object of study was to irradiate the polished surface of the surfacing with a pulsed electron beam using the SOLO facility [16]. The beam parameters were the following: accelerated electron energy of 17 keV, electron-beam energy density of 10 J/cm², pulse duration of 50 μs, number of pulses of 3, and pulse-repetition rate of 0.3 s⁻¹; the pressure of the residual gas (argon) in the working chamber of the installation was 0.02 Pa. The samples for TEM were prepared by the electrolytic thinning of plates cut parallel to the substrate surface from the upper part of the

surfacing metal. The fractures of the surfacing metal were studied using SEM.

RESULTS AND DISCUSSION

Analysis of the results obtained using SEM (Fig. 1) indicates that the surfacing metal of sample no. 1 has a pronounced layered structure (Fig. 1a) due to the technology of surfacing formation. The surfacing metal of sample no. 2 does not have a layered structure (Fig. 1b).

Layers and interlayer spaces can be distinguished by contrast and structure. The interlayer spaces are fragmented by a network of microcracks. It can be assumed that cracking occurs along the grain boundaries. It is known that the irradiation of metals and alloys with a pulsed electron beam can lead to the formation of tensile stresses in the surface layer, the relaxation of which can form microcracks [17]. Therefore, it can be assumed that the metal of the layers and interlayer spaces differs in their ability to relax elastic stresses arising in the material as a result of high-speed thermal action upon irradiation with a pulsed electron beam. The surfacing layers are characterized by a more dispersed structure and the absence of microcracks.

The elemental composition of the surfacing metal was studied using X-ray spectral analysis. The elemental composition of both surfacing layers and interlayer spaces was determined. An example of elemental analysis of the surfacing metal using the point-by-point method is shown in Figs. 2 and 3. The results of quantitative analysis of the elemental composition of the surfacing metal given in Tables 3 and 4 showed a significant difference in the composition of the layers and interlayer spaces. The surfacing layers in all samples (region 1) are significantly enriched with oxygen and do not contain nickel, which is present in the Sv-08GA wire (0.45 wt %). Nickel was found exclusively in the interlayer spaces (Table 1, region 2).

The fracture surface of the surfacing metal was studied using SEM. Characteristic images of the frac-

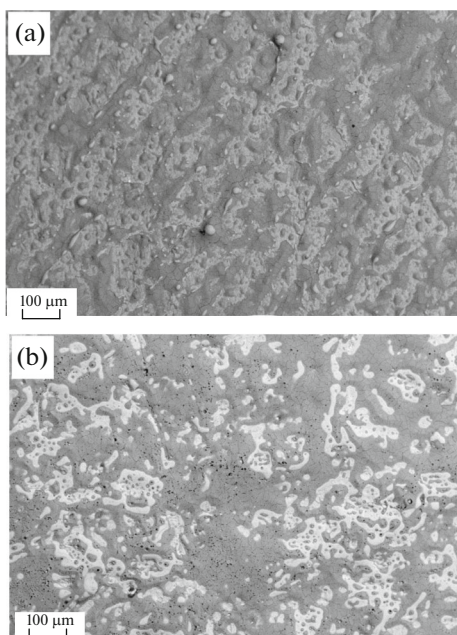


Fig. 1. Surface structure of the layer of surfaced metal of (a) sample 1 and (b) sample 2 subjected to polishing and subsequent irradiation with a pulsed electron beam.

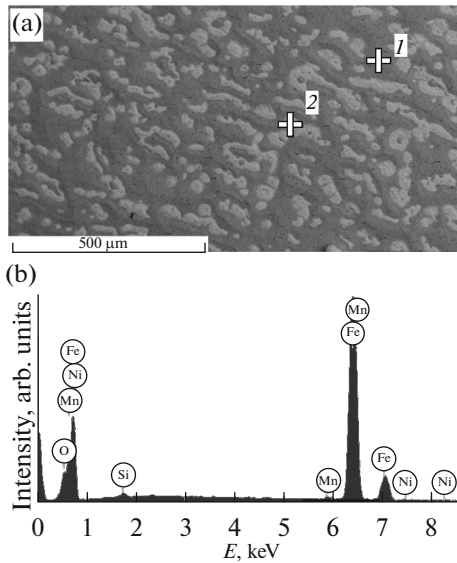


Fig. 2. (a) SEM image of the surface of the surfacing of sample no. 1 irradiated with a pulsed electron beam; (b) energy spectra obtained from area 2.

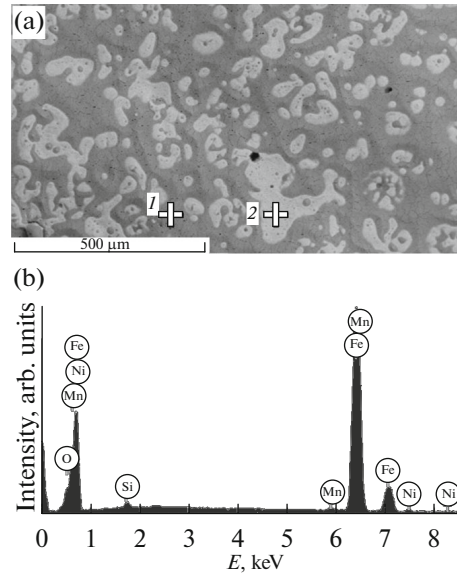


Fig. 3. (a) SEM image of the surface of the surfacing of sample no. 2 irradiated with a pulsed electron beam; (b) energy spectra obtained from area 2.

ture structure are shown in Fig. 4. It can be noted that the predominant mechanism for destruction of the surfacing metal is ductile destruction regardless of the sample. In this case, a pit structure characteristic of a ductile fracture is formed [18].

It is much less common to detect areas of quasi-brittle destruction of the surfacing material (Fig. 4, areas of quasi-brittle fracture are indicated by dark arrows). This type of destruction is characterized by a brook fracture.

Another element of the fracture structure of the surfacing metal are micropores and macropores, as well as discontinuities (Fig. 4, defects are indicated by white arrows). When analyzing the results of studying the fracture surface of the surfacing samples, it was noted that in sample no. 1 the number (per unit area of the fracture surface) of discontinuities, micropores and macropores of the surfacing metal is greater than in sample no. 2.

The phase composition and defect structure of the surfacing metal were studied using TEM [13–15, 19]. The phases that form the surfacing metal were identified by indexing electron-diffraction patterns and using methods for analyzing images obtained in the dark-field mode [19, 20]. It was established that the main phase of surfacing for all samples is the α phase. It is a solid solution based on the body-centered cubic (bcc) iron lattice and is a polycrystalline aggregate, i.e., has a granular structure. Grains of the α phase can be divided into three types according to the defect structure.

The first type includes grains, in the volume of which there is a subgrain (fragmented) structure. Fragment sizes range from 150 to 410 nm. The average size of grain fragments of the surfacing metal in sample no. 1 was 280 nm, and in sample no. 2 it was 300 nm. An analysis of the electron-diffraction patterns shows that, in most cases, the fragments are separated by low-angle boundaries, the misorientation of which varies within 1° – 3° . The second type are grains of the α phase, in the bulk of which no fragments were found. The third type are grains of the α phase, in the volume of which particles of iron carbide (cementite) of rounded shape were found (Fig. 5). The particle sizes of cementite are in the range from 20 to 80 nm. Such grains were found only in surfacing metal no. 2.

Dislocations are present in the volume of grains and fragments. Dislocations are distributed randomly or form a network structure.

Table 3. Results of X-ray spectral analysis of the areas of the surfacing metal of sample no. 1 indicated in Fig. 2a

Element	Area 1		Area 2	
	wt %	at %	wt %	at %
O	21.71	48.98	5.77	17.52
Si	0.65	0.84	0.54	0.94
Mn	1.00	0.66	0.81	0.72
Fe	76.63	49.53	92.09	80.17
Ni	0.0	0.0	0.79	0.65

Table 4. Results of X-ray spectral analysis of the areas of the surfacing metal of sample no. 2 indicated in Fig. 2a

Element	Area 1		Area 2	
	wt %	at %	wt %	at %
(O + C)	23.33	51.23	4.39	13.73
Si	0.76	0.95	0.79	1.41
Mn	1.08	0.69	0.95	0.87
Fe	74.83	47.13	92.97	83.23
Ni	0.00	0.00	0.90	0.77

The material under study is characterized by elastic stresses [21]. In studies of thin foils using electron microscopy, in this case, bending extinction contours are present in the images of the structure. The sources of stress fields are the interfaces between grains and subgrains (fragments), as well as inclusions of second phases.

Along with ferrite grains, pearlite grains were found in the surfacing metal. Pearlite has a lamellar structure. The relative content of pearlite grains in the surfacing of sample no. 1 is 15%, in the surfacing of sample no. 2 it is 45% of the metal structure.

Using well-known generally accepted methods for analyzing the structure of metals and alloys used in studying foils by electron microscopy [19, 22–24], the

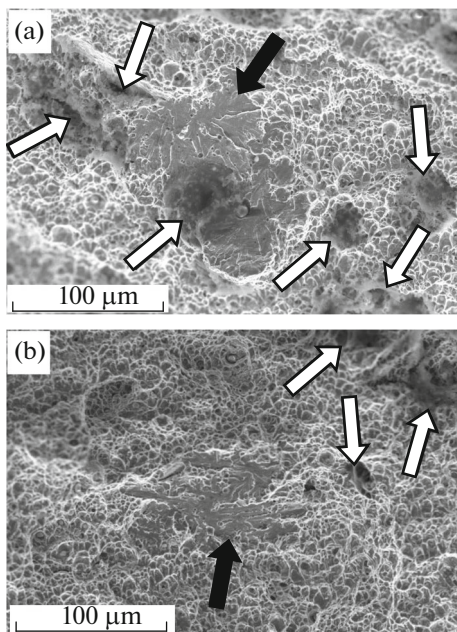


Fig. 4. SEM image of the fracture surface of the surfacing metal of (a) sample no. 1 and (b) sample no. 2. Light arrows indicate micropores and macropores, metal discontinuities; dark arrows indicate areas of quasi-brittle fracture.

relative content of pearlite grains and ferrite grains (δ), the values of the scalar (ρ) and excess (ρ_{\pm}) dislocation densities, and amplitude of curvature–torsion (the value proportional to the values of internal long-range stress fields) of a local area of the foil metal (χ) were determined. The results of measurements for samples no. 1 and no. 2 are given in Table 5. The analysis showed that the main volume of surfacing, regardless of the sample, is made up of ferrite grains: 0.85 of the surfacing volume in sample no. 1 and 0.55 in sample no. 2. The relative content of pearlite grains in surfacing no. 2 is three times higher than in surfacing no. 1, which is due to the use of carbon–fluorine containing additives in the formation of surfacing no. 2. The main volume of ferrite grains (0.75 in surfacing no. 1 and 0.3 in surfacing no. 2) is fragmented for all samples. There are dislocations in the volume of ferrite and pearlite grains; the value of the scalar dislocation density averaged over all structural components of the material in surfacing no. 2 is 1.24 times higher than in surfacing no. 1. The highest values of the scalar dislocation density were found in surfacing no. 1 in pearlite grains and in surfacing no. 2 in grains of unfragmented ferrite. The value of the excess dislocation density in surfacing no. 2 is 1.32 times higher than in surfacing no. 1. The largest value of the excess dislocation density, regardless of the sample, is reached in the grains of unfragmented ferrite. The curvature–torsion amplitude in surfacing no. 2 is 3.8 times higher than in surfacing no. 1. In the most stressed state in surfacing no. 1, there are grains of unfragmented ferrite; in surfacing no. 2, there are grains of fragmented ferrite. Comparing the characteristics of the dislocation structure of ferrite grains, it can be noted that, regardless of the sample, the lowest values of the scalar and excess dislocation densities

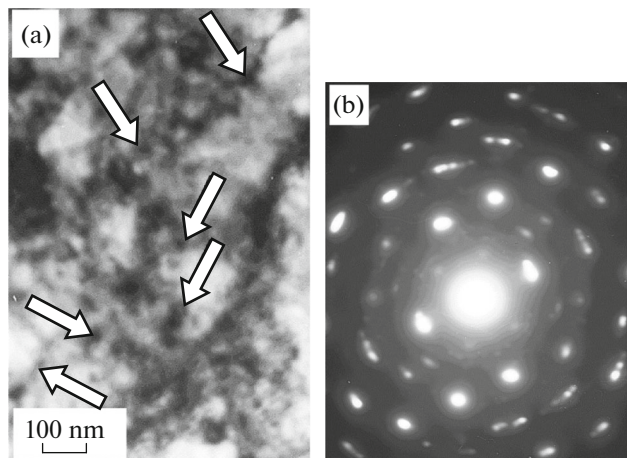


Fig. 5. (a) TEM image of grains of the α phase of surfacing no. 2 containing nanoscale rounded iron-carbide particles in the bright-field mode, arrows indicate particles of the carbide phase; (b) electron-diffraction pattern.

Table 5. Characteristics of the defect structure of the surfacing samples no. 1 and no. 2

Parameters of the structure	Pearlite		Unfragmented ferrite		Fragmented ferrite		Ferrite–carbide mixture		On average by material	
	no. 1*	no. 2*	no. 1	no. 2	no. 1	no. 2	no. 1	no. 2	no. 1	no. 2
Volume fraction	0.15	0.45	0.1	0.15	0.75	0.3	No	0.1		
$\rho, \times 10^{10} \text{ cm}^{-2}$	3.23	2.79	2.35	3.32	1.75	1.47	No	3.23	2.03	2.52
$\rho_{\pm}, \times 10^{10} \text{ cm}^{-2}$	1.94	2.8	2.02	3.22	1.74	1.32	No	2.42	1.8	2.38
$\chi, \text{ cm}^{-1}$	485	700	505	805	435	3290	No	2880	450	1710

* characteristics of the metal of surfacing no. 1 and surfacing no. 2.

were found in grains of fragmented ferrite. Obviously, this is due to the rearrangement of the dislocation structure and the departure of some of the dislocations to the low-angle boundaries of the fragments.

CONCLUSIONS

SEM and TEM methods were used to study the phase composition, defect structure, and fracture surface of metal surfaced on steel using Sv-08GA wire under a flux layer of silicomanganese slag with a low content of manganese oxide (sample no. 1) and a carbon–fluorine containing additive (sample no. 2). It was established that the surfacing metal has a layered structure most pronounced in surfacing no. 1.

It was revealed that the predominant mechanism of surfacing destruction is ductile fracture. Regions of quasi-brittle fracture are present much less frequently. It was shown that the main structural components (regardless of the sample) are grains of the α phase of the surfacing metal, i.e., grains of a solid solution based on the crystalline bcc lattice of iron. The second structural component of the surfacing are pearlite grains of lamellar morphology, the relative content of which in surfacing no. 2 is three times higher than in surfacing no. 1. In most cases (regardless of the sample), the α -phase grains are fragmented. The values of the scalar and excess dislocation densities were estimated. It was shown that surfacing no. 2 is characterized by higher values of the scalar and excess dislocation densities and amplitudes of curvature–torsion of local sections of the foil.

Thus, the results obtained in the study show that the use of a carbon–fluorine containing additive in the formation of a surfacing layer by electric-arc surfacing using Sv-08GA wire under a flux layer of silicomanganese slag with a low content of manganese oxide has a significant effect on the phase composition and defect substructure of the surfaced metal. Obviously, this, in turn, will affect the strength and tribological properties of the surfacing material.

CONFLICT OF INTEREST

We declare that we have no conflict of interest.

REFERENCES

1. Yu. Ivanov, A. Teresov, V. Gromov, S. Konovalov, V. Kormyshev, and K. Aksenova, *Mater. Sci. Technol.* **33**, 2040 (2017).
<https://doi.org/10.1080/02670836.2017.1343231>
2. E. V. Kapralov, S. V. Raykov, E. A. Budovskikh, V. E. Gromov, E. S. Vashchuk, and Yu. F. Ivanov, *Bull. Russ. Acad. Sci.: Phys.* **78**, 1015 (2014).
<https://doi.org/10.3103/S1062873814100098>
3. V. E. Gromov, E. V. Kapralov, S. V. Raikov, Yu. F. Ivanov, and E. A. Budovskikh, *Usp. Fiz. Met.*, No. 4, 211 (2014).
4. S. V. Raikov, E. V. Kapralov, E. S. Vashchuk, E. A. Budovskikh, V. E. Gromov, Yu. F. Ivanov, and K. V. Sosnin, *Uprochnyayushchie Tekhnol. Pokrytiya*, No. **122**, 40 (2015).
5. E. V. Kapralov, E. A. Budovskikh, V. E. Gromov, and Yu. F. Ivanov, *Russ. Phys. J.* **58**, 471 (2015).
6. N. A. Kozyrev, A. A. Umanskii, R. E. Kryukov, P. D. Sokolov, and L. V. Dumova, *Proizvod. Prokata*, No. 9, 33.
7. N. A. Kozyrev, R. E. Kryukov, N. E. Kryukov, A. A. Usol'tsev, and A. R. Mikhno, *Teor. Tekhnol. Metall. Proizvod.*, No. 26, 17 (2018).
8. N. A. Kozyrev, R. E. Kryukov, N. E. Kryukov, I. N. Koval'skii, and A. A. Usol'tsev, *Zagotovitel'nye Proizvod. Mashinostr.*, No. 6, 249 (2017).
9. N. A. Kozyrev, R. E. Kryukov, O. E. Kozyreva, E. A. Zernin, D. S. Kartsev, *IOP Conf. Ser.: Mater. Sci. Eng.* **132**, 1 (2016).
<https://doi.org/10.1088/1757-899X/142/1/012014>
10. R. E. Kryukov, N. A. Kozyrev, A. A. Usoltsev, and O. E. Kozyreva, in *Proc. International Scientific and Research Conference on Knowledge-Based Technologies in Development and Utilization of Mineral Resources* (2017), Vol. 4, p. 1.
11. Yu. F. Ivanov, R. E. Kryukov, V. E. Gromov, N. A. Kozyrev, and Yu. A. Rubannikova, *Fundam. Probl. Sovrem. Materialoved.* **18**, 265 (2021).
<https://doi.org/10.25712/ASTU.1811-1416.2021.03.002>

12. R. E. Kryukov, N. A. Kozyrev, V. E. Gromov, A. M. Glezer, Yu. F. Ivanov, and Yu. A. Rubannikova, *Deform. Razrushenie Mater.*, No. 11, 10 (2021).
13. F. R. Egerton, *Physical Principles of Electron Microscopy* (Springer, Basel, 2016).
14. C. S. S. R. Kumar, *Transmission Electron Microscopy: Characterization of Nanomaterials* (Springer, New York, 2014).
15. C. B. Carter and D. B. Williams, *Transmission Electron Microscopy* (Springer, Berlin, 2016).
16. *Electron-Ion-Plasma Modification of the Surface of Non-ferrous Metals and Alloys*, Ed. by N. N. Koval' and Yu. F. Ivanov (NTL, Tomsk, 2016) [in Russian].
17. V. P. Rotshtein, D. I. Proskurovskii, G. E. Ozur, and Yu. F. Ivanov, *Modification of Surface Layers of Metallic Materials by Low-Energy High-Current Electron Beams* (Nauka, Novosibirsk, 2017) [in Russian].
18. *Metals Handbook: Fractography and Atlas Fractographs* (Am. Soc. Met., 1982).
19. L. M. Utevsii, *Diffraction Electron Microscopy in Metal Science* (Metallurgiya, Moscow, 1973) [in Russian].
20. K. W. Andrews, D. J. Dyson, and S. R. Keown, *Interpretation of Electron Diffraction Patterns* (Springer, New York, 1967; Mir, Moscow, 1971).
21. P. Hirsch, A. Howie, R. Nicholson, D. Pashley, and M. Whelan, *Electron Microscopy of Thin Crystals* (Butterworths, London, 1965; Mir, Moscow, 1967).
22. K. S. Chernyavskii, *Stereology in Physical Metallurgy* (Metallurgiya, Moscow, 1977) [in Russian].
23. N. A. Koneva, E. V. Kozlov, L. I. Trishkina, and D. V. Lychagin, in *Proc. Int. Conf. on New Methods in Physics and Mechanics of a Deformable Solid Body* (Tomsk. Gos. Univ., Tomsk, 1990), p. 83.
24. V. E. Gromov, E. V. Kozlov, V. I. Bazaikin, V. Ya. Tsell-ermaer, Yu. F. Ivanov, et al., *Physics and Mechanics of Drawing and Forging* (Nedra, Moscow, 1997) [in Russian].

Translated by S. Rostovtseva